EduChemia
Jurnal Kimia dan Pendidikan

Vol.10, No.1, 2025, p. 39-52
e-ISSN 2502-4787

PHOSPHATE ACCUMULATION USING MgO-Fe_3O_4/AGAROSE/OXALIC ACID GEL AS A DIFFUSIVE GRADIENT IN THIN FILMS (DGT) BINDING LAYER

Layta Dinira[1*], Sullahudin Ahmad Rafif[2], Salwa Ulayya[2], Barlah Rumhayati[1], Darjito[1], Akhmad Sabarudin[1**]

[1]*Department of Chemistry, Faculty of Mathematics and Natural Sciences, Brawijaya University, Malang, Indonesia*
[2]*Undergraduate Student, Department of Chemistry, Faculty of Mathematics and Natural Sciences, Brawijaya University, Malang, Indonesia*

E-mail: *laytadinira@ub.ac.id; **sabarjpn@ub.ac.id

Received: 11 Oktober 2024. Accepted: 17 April 2025. Published: 30 April 2025

DOI: 10.30870/educhemia.v10i1.29113

Abstract: Monitoring the phosphate concentration in water is critical because excessive phosphate can lead to the death of aquatic organisms. Phosphate can be monitored via a passive sampler called the diffusion gradient in thin films (DGT). This study combines MgO and Fe_3O_4 impregnated in agarose crosslinked with oxalic acid to accumulate phosphate from the solution as a DGT binding gel. The parameters observed in this study were the MgO/Fe_3O_4 mass ratio (1:3, 1:1, 3:1), accumulation time (20, 40, 60, 120, 240, and 1440 min), phosphate concentration (0.2, 0.4, 0.6, 0.8, and 1 mg/L) and pH (4, 5, 6, 7, and 8) for phosphate accumulation. The XRD patterns confirmed that the adsorbents used were MgO and Fe_3O_4. SEM analysis revealed that the gel had an average pore size of 31.78 µm, and the adsorbents were evenly distributed. Gels with a MgO/Fe_3O_4 mass ratio of 3:1 can adsorb up to 97.19 ± 0.36% of the phosphate. The phosphate accumulation reached an optimum after a minimum adsorption time of 4 h and when the phosphate concentration in the solution was 0.4 mg/L. The pH of the solution had no significant effect on phosphate accumulation. This study revealed that MgO-Fe_3O_4/agarose/oxalic acid gel is an excellent binding gel for the accumulation of phosphate from water.

Keywords: DGT; MgO; Fe_3O_4; agarose; oxalic acid

Abstrak: Pemantauan fosfat dalam perairan sangat penting karena kadar fosfat berlebih dapat mengakibatkan eutrofikasi yang berujung pada kematian organisme air. Pemantauan kadar fosfat dalam perairan dapat menggunakan *passive sampler* yang dinamakan *Diffusive Gradient in Thin Films* (DGT). Penelitian ini mengombinasikan MgO dan Fe_3O_4 terimpregnasi dalam gel agarosa terikat silang asam oksalat untuk mengakumulasi fosfat dari larutan sebagai gel pengikat DGT. Parameter-parameter yang diamati pada penelitian ini adalah pengaruh rasio massa MgO/Fe_3O_4 (1:3; 1:1; 3:1), waktu akumulasi (20; 40; 60; 120; 240; dan 1440 menit), konsentrasi fosfat dalam larutan (0,2; 0,4; 0,6; 0,8; dan 1 mg/L) dan pH larutan (4; 5; 6; 7; dan 8) terhadap akumulasi

fosfat. Hasil penelitian menunjukkan bahwa puncak-puncak yang teramati pada XRD mengonfirmasi bahwa adsorben yang digunakan adalah MgO dan Fe_3O_4. Hasil SEM menunjukkan bahwa gel memiliki ukuran pori rata-rata sebesar 31,78 μm dan adsorben terdistribusi merata. Gel dengan rasio massa MgO/Fe_3O_4 sebesar 3:1 dapat mengadsorpsi fosfat hingga 97,19 ± 0,36%. Akumulasi fosfat mencapai optimum setelah adsorpsi minimal selama 4 jam dan ketika konsentrasi fosfat dalam larutan sebesar 0,4 mg/L. pH larutan tidak berpengaruh signifikan terhadap akumulasi fosfat. Penelitian ini menunjukkan bahwa gel MgO-Fe_3O_4/agarosa/asam oksalat dapat mengakumulasi fosfat dari perairan dengan sangat baik.

Kata kunci: fosfat; MgO; Fe_3O_4; agarosa; asam oksalat

INTRODUCTION

Phosphate (PO_4^{3-}) is an essential chemical for natural biological life. Agriculture uses phosphate as a fertilizer (Puspitasari et al., 2018; Sumbayak & Gultom, 2020). However, excess phosphate can lead to eutrophication, which results in excessive zooplankton growth and proliferation (Badamasi et al., 2019).

According to the Government Regulation of the Republic of Indonesia Number 22 of 2021, phosphate is one of the factors contributing to water pollution in irrigation water and must not exceed 0.1 mg/L (Pemerintah Republik Indonesia, 2022). Thus, monitoring phosphate levels in water is critical for preventing water contamination.

The grab sampling method can determine phosphorus levels in water (Udianto et al., 2022). However, sample analysis in the laboratory using the grab sampling method still requires analyte preconcentration, which might lead to errors in measurement. The diffusive gradient in thin films (DGTs) is a great and straightforward in situ measurement technique (Zheng et al., 2023). It is frequently used to assess aquatic species such as phosphorus (P), sulfur (S), arsenic (As), and metals. A DGT passive sampler consists of a binding layer, a diffusive layer, and a filter membrane (Li et al., 2019; Yabuki et al., 2014). Various phosphate binder layers have been utilized, including zirconium oxide, magnetite, ferihydrite, and $Mg(OH)_2$ (Maimulyanti et al., 2018; Sun et al., 2013; F. Xie et al., 2020; Y. Zhang et al., 2018).

The use of magnetite as a binding agent is based on its high affinity for phosphate ions (Shahid et al., 2019). Similar research on the use of Fe_3O_4 as a binding agent in DGTs was conducted by Zhang (Y. Zhang et al., 2018). Fe_3O_4 was used as a suspension. However, owing to the high affinity of Fe_3O_4 for phosphate ions, the phosphate concentration measured via DGT was three times greater than the actual phosphate concentration. Therefore, the use of Fe_3O_4 to adsorb phosphate in DGTs must be reduced and replaced with

another binding agent. Mg-based adsorbents are one of the available options. According to (F. Xie et al., 2020), $Mg(OH)_2$ adsorbs up to 21.37 μg of phosphate per disc binding gel DGT.

The existing studies only used a single binding agent to adsorb the analyte. There has never been a study of DGT-binding gels that use two binding agents to adsorb phosphate. Combining a Mg-based adsorbent with Fe_3O_4 is expected to reduce the high affinity of Fe_3O_4 in adsorbing phosphate without reducing the excellent phosphate adsorption percentage (~100%).

The DGT-binding gel used a hydrogel as the binding agent matrix. Polyacrylamide and agarose are commonly used as hydrogels for DGTs (H. Zhang & Davison, 1999). However, agarose, unlike polyacrylamide, is an environmentally friendly hydrogel (Date et al., 2020). This biopolymer can form crosslinks with other compounds because its structure is rich in hydroxyl groups (Jiang et al., 2023; Zucca et al., 2016). It is also safer to prepare and can withstand a pH range of 0–14 (Abolghasemi et al., 2016). The pore size can be adjusted by adjusting the crosslinker concentration (Popescu et al., 2022). Adding crosslinkers also increases the mechanical strength of hydrogels (Zheng et al., 2023).

Oxalic acid is an environmentally friendly dicarboxylate group that can be used as a crosslinker. The structure of oxalic acid consists of two –COOH groups that can form ionic interactions with the helix bonds of biopolymer hydrogel groups. Oxalic acid can form interconnected pores and reduce the pore size of a hydrogel (Popescu et al., 2022).

The ability of the DGT-binding gel to adsorb phosphate must be considered. Several factors can affect phosphate adsorption, such as the mass ratio of the binding agent, adsorption time, pH, and initial concentration of the solution. Therefore, this study developed and optimized the adsorption of phosphate using MgO-Fe_3O_4/agarose/oxalic acid gel.

METHOD

Materials and Apparatus

The chemicals used include $FeSO_4.7H_2O$ (p.a.), $FeCl_3.6H_2O$ (p.a.), 25% NH_4OH solution (p.a.), agarose (p.a.), oxalic acid (p.a.), MgO (p.a.), KH_2PO_4 (p.a.), ammonium heptamolybdate (p.a.), $SnCl_2$ (p.a.), H_2SO_4 98% (p.a.), glycerol (p.a.), phenolphthalein (PP) indicator, and HNO_3 solution.

The apparatus used to support the research included glassware, universal pH, micropipettes, circular molds with a

diameter of 2.5 cm, gel molds (Figure 1), a UV–Vis spectrophotometer (Thermo Scientific Genesys 10S), X-ray diffraction (PANalytical X'Pert PRO), and scanning electron microscopy (FEI Inspect S50).

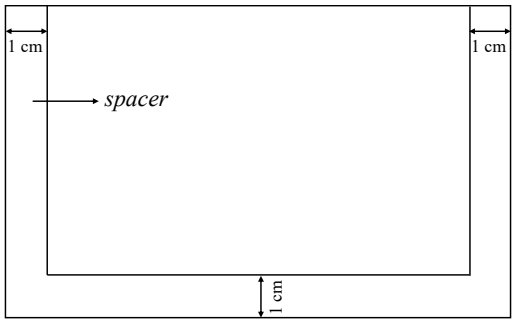

Figure 1. The gel mold consists of two pieces of glass (16 x 10 cm). A Teflon spacer formed like the letter U was placed in the middle of the mold. The two pieces of glass and the spacer were clamp with a clip.

Synthesis of Fe_3O_4

$FeSO_4.7H_2O$ (2.78 grams) and $FeCl_3.6H_2O$ (5.41 grams) were put into a glass beaker and dissolved in 50 mL of distilled water with a magnetic stirrer for approximately 10 minutes until homogeneous. Moreover, 3 M NH4OH was added to the solution using a syringe pump at 50 mL/hour until the pH reached 10. The precipitate was washed with distilled water until it reached pH 7 and dried in an oven at 60 °C for 1.5 hours.

Synthesis of MgO-Fe_3O_4/Agarose/Oxalic Acid Gel

Oxalic acid (0.015 grams) was dissolved in 3 mL of distilled water. The solution was added to a glass beaker containing MgO and transferred to another glass beaker containing Fe_3O_4. The mixture was stirred until homogenous.

Distilled water (7 mL) was added to 0.150 grams of agarose and stirred until the agarose completely dissolved. If the agarose did not dissolve completely, the mixture was heated on a hot plate until a clear, colorless solution formed. The agarose mixture was poured into a beaker containing an oxalic acid-MgO-Fe_3O_4 mixture when the temperature of the agarose mixture was 60 °C. The solution was stirred until homogeneous and then pipetted into a mold (Figure 1). The mold was placed in an oven at 40 °C for 15 minutes.

The gel was cooled at room temperature for approximately 15 minutes. The gel was cut using a circular mold with a diameter of 2.5 cm, immersed in distilled water, and stored for a minimum of 24 hours before use. The thickness of the gel after storage for 24 hours was measured. Gels with a MgO:Fe_3O_4 mass ratio of 3:1 were characterized by scanning electron microscopy (FEI Inspect S50).

Effect of the MgO/Fe_3O_4 mass ratio on phosphate accumulation

Three gels with different MgO/Fe_3O_4 mass ratios (1:0; 3:1; 1:1; 1:3; and 0:1) were

each put into an Erlenmeyer flask containing 15 mL of 2 mg/L phosphate solution. Phosphate adsorption was performed by shaking the phosphate solution containing the gel for 24 hours on a shaker at 100 rpm. After 24 h, the solution was filtered, and the gel and filtrate were obtained.

Effect of adsorption time on phosphate accumulation

Three gels with the optimum MgO/Fe_3O_4 mass ratio were placed into an Erlenmeyer flask containing 15 mL of 2 mg/L phosphate solution. The gels and the phosphate solution were shaken for 20, 40, 60, 120, 240, and 1440 minutes at 100 rpm. The solution was filtered to obtain the gel and filtrate.

Effect of Phosphate Concentration on Phosphate Accumulation

Three gels with the optimum MgO/Fe_3O_4 mass ratio were put into an Erlenmeyer flask containing 15 mL of phosphate solution at concentrations of 0.2, 0.4, 0.6, 0.8, and 1 mg/L and then shaken for 24 hours at 100 rpm. Filtration was used to separate the gel and filtrate.

Effect of pH on Phosphate Accumulation

Three gels with the optimum MgO/Fe_3O_4 mass ratio were put into an Erlenmeyer flask containing 15 mL of 0.4 mg/L phosphate solution with a pH of 4–8 (adjusted with HNO_3 and NaOH) and then shaken at 100 rpm for 24 hours. The solution was filtered to obtain a gel and filtrate.

Data analysis

The crystallite diameter of the binding agent was calculated using the Debye–Scherrer equation, as shown below:

$$D = \frac{K\lambda}{\beta cos\theta} \quad (2)$$

β is the FWHM (full width at half maximum or half width) (in radians), θ is the position of the maximum diffraction peak, K is Scherrer's constant of 0.9, and λ is the X-ray wavelength (1.5406 Å or 0.15406 nm).

The initial phosphate concentration before and after adsorption was analyzed using the Stannous Chloride method. The phosphate concentration was converted into the phosphate mass before (m_o) and after adsorption (m_t). The phosphate accumulation (%) was calculated using the equation below:

$$\text{Phosphate accumulation (\%)} = \frac{m_o - m_t}{m_o} \times 100\% \quad (1)$$

The phosphate accumulation obtained for each variation was analyzed using one-way ANOVA followed by Tukey's test at the 95% confidence level ($p \leq 0.05$).

RESULTS AND DISCUSSION

Characterization of the MgO-Fe_3O_4/Agarose/Oxalic Acid Gel

The synthesis of $FeSO_4.7H_2O$ and $FeCl^3.6H_2O$ (mole Fe^{2+}:Fe^{3+} = 1:2) produced a black precipitate. The precipitate was washed to pH 7, dried, and characterized using XRD. Figure 2 shows that the precipitate was Fe_3O_4 because there were peaks at 30°, 35°, 43°, 54°, 57°, and 63°, which is the typical 2θ of Fe_3O_4. These peaks indicated the (220), (311), (400), (422), (511), and (440) fields (Bertolucci et al., 2015). The Debye–Scherrer equation calculation revealed that the average diameter of the Fe_3O_4 crystallites (D) was 19.08 nm.

Figure 3 shows the XRD characterization of the MgO used in this study. The XRD pattern indicated typical MgO angles at 36°, 42°, 62°, 74°, and 78°, which correspond to the (111), (200), (220), (311), and (222) planes, respectively, according to the reference standard document (JCPDS 98-015-9369) (Demirci et al., 2021; Salman et al., 2021). The average crystallite diameter of MgO (D) determined using the Debye–Scherrer equation was 71.76 nm.

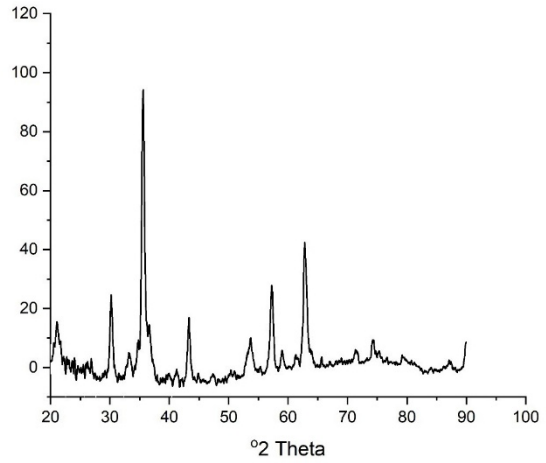

Figure 2. XRD pattern of Fe_3O_4

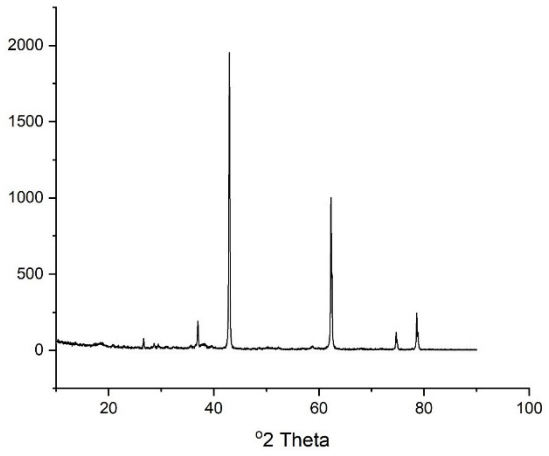

Figure 3. XRD pattern of MgO

The MgO and Fe_3O_4 were impregnated into agarose crosslinked with oxalic acid gel and cut into a round shape with a diameter of 2.5 cm. The color of the gel was gray due to a mixture of white MgO and black Fe_3O_4. It had a thickness of 0.5 mm. A binding gel of this size can be inserted into the DGT passive sampler with a total layer thickness of 1.34 mm (Davison, 2016).

Dinira et al. (2024) crosslinked agarose with oxalic acid. The IR spectrum of

agarose-oxalic acid revealed a new peak at 1727 cm^{-1} that was not present in the IR spectrum of agarose. This suggests that agarose was successfully crosslinked with oxalic acid via an esterification reaction.

The gel was stored in distilled water for 24 hours. During storage, the distilled water was changed three times. The MgO/Fe_3O_4/agarose oxalic acid gel was characterized using SEM to evaluate the pore size and binding agent distribution of the gel. Figure 4 shows the surface of the gel. The white areas indicate that MgO and Fe_3O_4 were found and spread well in the gel matrix. The average pore size of the gel was 31.78 µm.

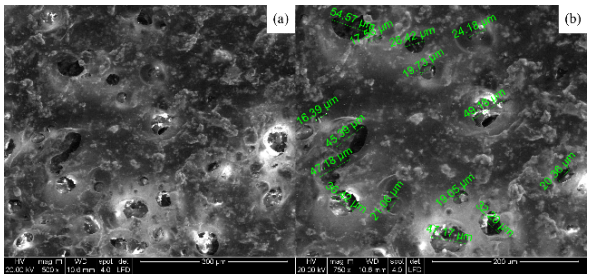

Figure 4. SEM image of MgO/Fe_3O_4 3:1 impregnated in agarose-oxalic acid gel

Effect of the MgO/Fe_3O_4 mass ratio on the phosphate accumulation in the MgO/Fe3O4/agarose/oxalic acid gel

The accumulation of phosphate in MgO/Fe_3O_4/agarose/oxalic acid gels of various mass ratios is shown in Figure 5. All the gels accumulated more than 90% phosphate. The highest phosphate accumulation was obtained when the gel containing only Fe_3O_4 was used (98.09 ± 0.44%).

The pH of the phosphate solution used in this study was 6.13. At pH values greater than 4.6, Fe_3O_4 is negatively charged (Zhu et al., 2015) and repels phosphate, decreasing its accumulation. The high degree of phosphate accumulation is due to the high affinity of Fe^{3+} in Fe_3O_4 for phosphate (Senn et al., 2015). The high phosphate accumulation in the gel contained only MgO (97.5 ± 0.35%), which was attributed to the positively charged MgO surface at pH < 9.2 (Ismail et al., 2022). The positively charged MgO surface can adsorb phosphate via electrostatic interactions (Wang et al., 2024).

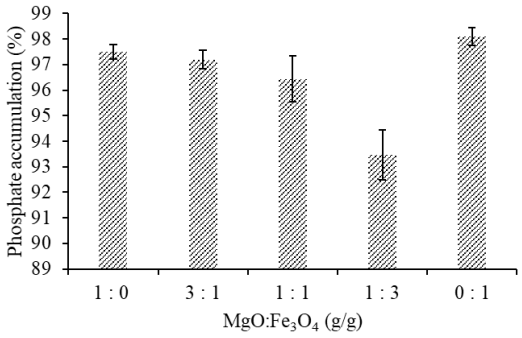

Figure 5. Effect of binding agent mass ratio on phosphate accumulation

According to the statistical test, phosphate accumulation in the gel was not significantly different from that in the gel containing only MgO or the gel containing MgO/Fe_3O_4 at a 3:1 ratio. (97.19 ±

0.36%). This result demonstrates that when Fe_3O_4 is replaced with MgO, the gel can still adsorb phosphate effectively. However, iron oxide has a strong ability to attract phosphate; thus, it is still required to adsorb phosphate (Z. Zhang et al., 2020). As a result, the MgO/Fe_3O_4/agarose/oxalic acid gel at a 3:1 ratio was used to determine the effect of adsorption time.

Effect of Adsorption Time on Phosphate Accumulation in MgO/Fe_3O_4/Agarose/oxalic acid gels

Figure 6 shows phosphate accumulation on a MgO/Fe_3O_4/agarose/oxalic acid gel with an optimal MgO/Fe_3O_4 mass ratio over time. Phosphate accumulated quickly in the first 60 min (92.21 ± 6.49%). Figure 5 also shows that as the contact time between the binding gel and the phosphate solution increased, the amount of phosphate adsorbed increased until the optimal conditions were reached.

The study revealed that phosphate adsorption was most effective after 4 h (98.40 ± 0.05%) and remained constant for 24 h (98.73 ± 0.95%). This phenomenon suggests that equilibrium has been attained after at least 4 hours of adsorption (Saleh, 2022). The gel saturation in this study was achieved faster than that of the binding gel, which only used $Mg(OH)_2$. The accumulation of phosphate by $Mg(OH)_2$ slowed after 20 hours of adsorption (F. Xie et al., 2020).

Statistical tests revealed a p value (0.00) < α = 0.05, indicating a significant effect of adsorption time on phosphate accumulation in the gel. However, the statistical test revealed no significant difference between 60 and 1440 minutes. There were some fluctuations between 60 and 240 minutes. As a result, 4 hours was determined to be the minimum period for phosphate adsorption by the MgO/Fe_3O_4/agarose/oxalic acid gel.

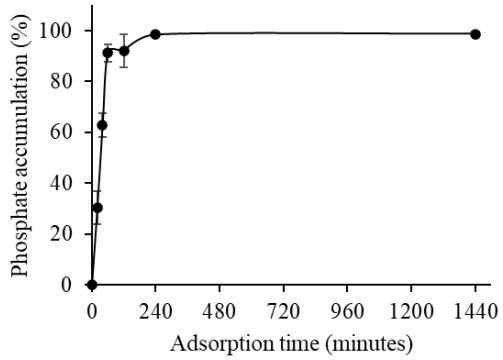

Figure 6. Effect of adsorption time on phosphate accumulation

Effect of Initial Solution Concentration on Phosphate Accumulation in MgO/Fe_3O_4/Agarose/Acid Oxalate Gels

The effect of the initial solution concentration on the accumulation of phosphate in the gel is shown in Figure 7. The optimum phosphate accumulation was reached when a phosphate solution with a

concentration of 0.4 mg/L was used (95.54 ± 1.99%). The degree of phosphate accumulation tended to be constant until the concentration reached 1 mg/L (93.68 ± 2.12%). The greater the amount of phosphate available in the solution is, the greater the degree of phosphate adsorption by the gel until the optimum conditions are reached. A higher concentration of phosphate solution in the solution provides a stronger driving force for the migration of phosphate from the solution to the gel surface (Du et al., 2022) so that the active sites of the gel can adsorb more phosphate. However, the amount of phosphate accumulated tends to be constant after the optimum conditions are reached because the active sites of the gel are saturated (Saefumillah & H, 2015).

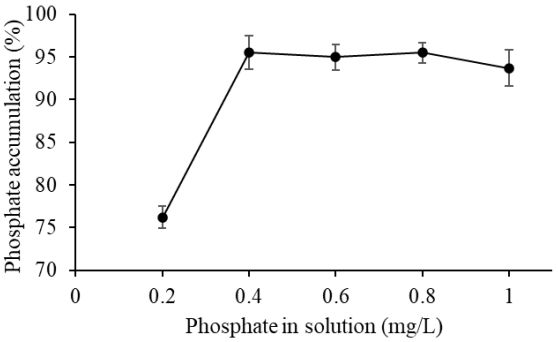

Figure 7. Effect of initial concentration of phosphate in solution on phosphate accumulation

Statistical tests revealed a p value (0.00) < α = 0.05. It can be concluded that the initial concentration of a solution significantly affects phosphate accumulation. The amount of phosphate accumulation decreased when the gel adsorbed phosphate from a solution with a one mg/L phosphate concentration. However, statistical tests revealed no significant difference in the amount of phosphate accumulated from phosphate solutions with concentrations ranging from 0.4 to 1 mg/L. Therefore, a phosphate concentration of 0.4 mg/L was used as the solution for the next variation.

Effect of Solution pH on Phosphate Accumulation in MgO/Fe_3O_4/Agarose/Oxalic Acid Gel

Figure 8 shows the effect of solution pH on phosphate accumulation in the gel. At pH 4–8, phosphate accumulation is relatively constant (approximately 90%). A pH of 6 resulted in maximum phosphate accumulation (93.35 ± 1.78%). At pH 6, the phosphate in the solution is in the form of $H_2PO_4^-$ (J. Xie et al., 2014), whereas MgO, an adsorbent with a relatively high mass, is positively charged, attracting $H_2PO_4^-$ ions to the gel. At pH 8, phosphate in solution begins to appear as HPO_4^{2-}; at higher pH values, the surface of Fe_3O_4 gradually converts to FeO^- (Karunanayake et al., 2019). The negative charges of HPO_4^{2-} and FeO^- resist each other, reducing phosphate accumulation.

Statistical tests revealed no significant effect of pH on phosphate accumulation (p value = 0.426, α = 0.05). This suggests that the gel can adsorb phosphate in waters with a pH of 4–8. The gel developed in this study has a lower pH range than the DGT binding gel, which contains only $Mg(OH)_2$. The $Mg(OH)_2$ binding gel can be deployed at pH 2–10 (F. Xie et al., 2020).

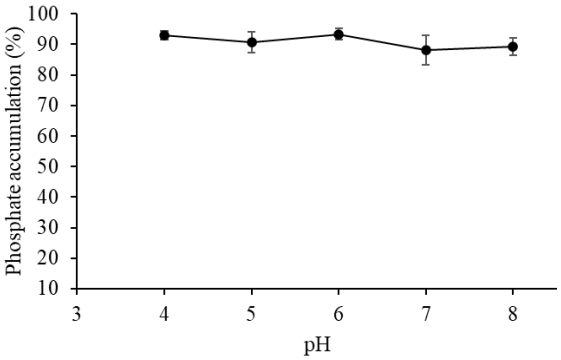

Figure 8. Effect of solution pH on phosphate accumulation

CONCLUSION

The critical finding of this study is that the MgO-Fe_3O_4/agarose/oxalic acid gel, as a binding gel, accumulates up to 100% phosphate. The mass ratio of MgO:Fe_3O_4, adsorption time, and initial concentration of the phosphate solution significantly affect the accumulation of phosphate by the MgO-Fe_3O_4/agarose/oxalic acid gel. Optimal phosphate adsorption occurred when a gel with a MgO/Fe_3O_4 mass ratio of 3:1, a minimum adsorption time of 4 hours, and a phosphate content of 0.4 mg/L was used. Since phosphate accumulation in phosphate solutions at pH 4–8 tends to be constant, the gel can adsorb phosphate in water within this pH range. This study revealed that the MgO-Fe_3O_4/agarose/oxalic acid gel is an excellent binding gel for the accumulation of phosphate from water.

REFERENCES

Abolghasemi, M. M., Sobhi, M., & Piryaei, M. (2016). Preparation of a novel green optical pH sensor based on immobilization of red grape extract on bioorganic agarose membrane. *Sensors and Actuators, B: Chemical*, *224*, 391–395. https://doi.org/10.1016/j.snb.2015.10.038

Badamasi, H., Yaro, M. N., Ibrahim, A., & Bashir, I. A. (2019). Impacts of Phosphates on Water Quality and Aquatic Life. *Chemical Research Journal*, *4*(3), 124–133.

Bertolucci, E., Galletti, A. M. R., Antonetti, C., Marracci, M., Tellini, B., Piccinelli, F., & Visone, C. (2015). Chemical and magnetic

properties characterization of magnetic nanoparticles. *Conference Record - IEEE Instrumentation and Measurement Technology Conference*, *2015-July*, 1492–1496. https://doi.org/10.1109/I2MTC.2015.7151498

Date, P., Tanwar, A., Ladage, P., Kodam, K. M., & Ottoor, D. (2020). Biodegradable and biocompatible agarose–poly (vinyl alcohol) hydrogel for the in vitro investigation of ibuprofen release. *Chemical Papers*, *74*(6), 1965–1978. https://doi.org/10.1007/s11696-019-01046-8

Davison, W. (2016). *Diffusive Gradients in Thin-Films for Environmental Measurements*. Cambridge University Press.

Demirci, S., Yildirim, B. K., Tünçay, M. M., Kaya, N., & Güllüoğlu, A. N. (2021). Synthesis, characterization, thermal, and antibacterial activity studies on MgO powders. *Journal of Sol-Gel Science and Technology*, *99*(3), 576–588. https://doi.org/10.1007/s10971-021-05609-8

Dinira, L., Rumhayati, B., Andayani, U., & Mardiana, D. (2024). Effect of casting temperature on the swelling degree and water content of agarose crosslinked with oxalic acid as DGT diffusion layer. *AIP Conference Proceedings*, *3068*(1). https://doi.org/10.1063/5.0202031

Du, M., Zhang, Y., Wang, Z., Lv, M., Tang, A., Yu, Y., Qu, X., Chen, Z., Wen, Q., & Li, A. (2022). Insight into the synthesis and adsorption mechanism of adsorbents for efficient phosphate removal: Exploration from synthesis to modification. *Chemical Engineering Journal*, *442*, 136147. https://doi.org/10.1016/j.cej.2022.136147

Ismail, M., Jobara, A., Bekouche, H., Abd Allateef, M., Ben Aissa, M. A., & Modwi, A. (2022). Impact of Cu Ions removal onto MgO nanostructures: adsorption capacity and mechanism. *Journal of Materials Science: Materials in Electronics*, *33*(15), 12500–12512. https://doi.org/10.1007/s10854-022-08207-8

Jiang, F., Xu, X. W., Chen, F. Q., Weng, H. F., Chen, J., Ru, Y., Xiao, Q., & Xiao, A. F. (2023). Extraction, Modification and Biomedical Application of Agarose Hydrogels: A Review. *Marine Drugs*, *21*(5), 299. https://doi.org/10.3390/md21050299

Karunanayake, A. G., Navarathna, C. M., Gunatilake, S. R., Crowley, M.,

Anderson, R., Mohan, D., Perez, F., Pittman, C. U., & Mlsna, T. (2019). Fe3O4 Nanoparticles Dispersed on Douglas Fir Biochar for Phosphate Sorption. *ACS Applied Nano Materials*, *2*(6), 3467–3479. https://doi.org/10.1021/acsanm.9b00430

Li, C., Ding, S., Yang, L., Wang, Y., Ren, M., Chen, M., Fan, X., & Lichtfouse, E. (2019). Diffusive gradients in thin films: devices, materials and applications. *Environmental Chemistry Letters*, *17*(2), 801–831. https://doi.org/10.1007/s10311-018-00839-9

Maimulyanti, A., Budiawan, Saefumillah, A., & Suseno, H. (2018). Effect of pH and anion interferences on determination of orthophosphate speciation by diffusive gradient in thin film (DGT) technique. *Rasayan Journal of Chemistry*, *11*(3), 1222–1228. https://doi.org/10.31788/RJC.2018.1133057

Pemerintah Republik Indonesia. (2022). Peraturan Pemerintah Nomor 22 Tahun 2021 tentang Penyelenggaraan Perlindungan dan Pengelolaan Lingkungan Hidup. In *Peraturan Pemerintah*. Kementerian Sekretariat Negara Republik Indonesia.

Popescu, I., Constantin, M., Pelin, I. M., Suflet, D. M., Ichim, D. L., Daraba, O. M., & Fundueanu, G. (2022). Eco-Friendly Synthesized PVA/Chitosan/Oxalic Acid Nanocomposite Hydrogels Embedding Silver Nanoparticles as Antibacterial Materials. *Gels*, *8*(5). https://doi.org/10.3390/gels8050268

Puspitasari, H. M., Yunus, A., & Harjoko, D. (2018). Dosis Pupuk Fosfat Terhadap Pertumbuhan Dan Hasil Beberapa Jagung Hibrida. *Agrosains*, *20*(2), 34–39.

Saefumillah, A., & H, R. R. (2015). Pengembangan Metode DGT (Diffusive Gradient In Thin Film) dengan Binding Gel Fe-Al-Oksida dan Pengikat Silang N,N'-Methylenebisacrylamide untuk Penyerapan Fosfat dalam Air. *Jurnal Kimia VALENSI*, 20–25. https://doi.org/10.15408/jkv.v0i0.3597

Saleh, T. A. (2022). Kinetic models and thermodynamics of adsorption processes: classification. *Interface Science and Technology*, *34*, 65–97. https://doi.org/10.1016/B978-0-12-849876-7.00003-8

Salman, K. D., Abbas, H. H., & Aljawad, H. A. (2021). Synthesis and characterization of MgO nanoparticle via microwave and sol-gel methods. *Journal of Physics: Conference Series*, *1973*(1), 012104. https://doi.org/10.1088/1742-6596/1973/1/012104

Senn, A. C., Kaegi, R., Hug, S. J., Hering, J. G., Mangold, S., & Voegelin, A. (2015). Composition and structure of Fe(III)-precipitates formed by Fe(II) oxidation in water at near-neutral pH: Interdependent effects of phosphate, silicate and Ca. *Geochimica et Cosmochimica Acta*, *162*, 220–246. https://doi.org/10.1016/j.gca.2015.04.032

Shahid, M. K., Kim, Y., & Choi, Y. G. (2019). Adsorption of phosphate on magnetite-enriched particles (MEP) separated from the mill scale. *Frontiers of Environmental Science and Engineering*, *13*(5), 71–83. https://doi.org/10.1007/s11783-019-1151-2

Sumbayak, R. J., & Gultom, R. R. (2020). Pengaruh Pemberian Pupuk Fosfat dan Pupuk Organik. *Jurnal Darma Agung*, *2*, 253–268.

Sun, Q., Chen, Y., Xu, D., Wang, Y., & Ding, S. (2013). Investigation of potential interferences on the measurement of dissolved reactive phosphate using zirconium oxide-based DGT technique. *Journal of Environmental Sciences (China)*, *25*(8), 1592–1600. https://doi.org/10.1016/S1001-0742(12)60140-5

Udianto, F., Kriswandana, F., & Rachmaniyah. (2022). Pemetaan Kualitas Air Sungai di Kawasan Industri Ngingas Sidoarjo Ditinjau dari Parameter BOD dan TSS Tahun 2021. *Jurnal Higiene Sanitasi*, *1*, 31.

Wang, C. Y., Zhou, H. D., Wang, Q., Xu, B. X., & Zhu, G. (2024). Efficiency and mechanism of phosphate adsorption and desorption of a novel Mg-loaded biochar material. *Environmental Science and Pollution Research International*, *31*(3), 4425–4438. https://doi.org/10.1007/s11356-023-31400-z

Xie, F., Li, L., Sun, X., Hu, T., Song, K., Giesy, J. P., & Wang, Q. (2020). A novel Mg(OH)2 binding layer-based DGT technique for measuring phosphorus in water and sediment. *Environmental Science: Processes and Impacts*, *22*(2), 340–349. https://doi.org/10.1039/c9em00508k

Xie, J., Wang, Z., Lu, S., Wu, D., Zhang, Z., & Kong, H. (2014). Removal and

recovery of phosphate from water by lanthanum hydroxide materials. *Chemical Engineering Journal*, *254*, 163–170. https://doi.org/10.1016/j.cej.2014.05.113

Yabuki, L. N. M., Colaço, C. D., Menegário, A. A., Domingos, R. N., Kiang, C. H., & Pascoaloto, D. (2014). Evaluation of diffusive gradients in thin films technique (DGT) for measuring Al, Cd, Co, Cu, Mn, Ni, and Zn in Amazonian rivers. *Environmental Monitoring and Assessment*, *186*(2), 961–969. https://doi.org/10.1007/s10661-013-3430-x

Zhang, H., & Davison, W. (1999). Diffusional characteristics of hydrogels used in DGT and DET techniques. *Analytica Chimica Acta*, *398*, 329–340.

Zhang, Y., Song, J., Zhou, H., Zhang, Y., & Wang, G. (2018). Novel Fe3O4 nanoparticles-based DGT device for dissolved reactive phosphate measurement. *New Journal of Chemistry*, *42*(4), 2874–2881. https://doi.org/10.1039/c7nj04464j

Zhang, Z., Yu, H., Zhu, R., Zhang, X., & Yan, L. (2020). Phosphate adsorption performance and mechanisms by nanoporous biochar–iron oxides from aqueous solutions. *Environmental Science and Pollution Research*, *27*(22), 28132–28145. https://doi.org/10.1007/s11356-020-09166-5

Zheng, S., Sheng, F., Gu, C., Li, Y., Fang, Z., & Luo, J. (2023). DGT method for the in situ measurement of triazines and the desorption kinetics of atrazine in soil. *Environmental Science and Pollution Research*, *30*(17), 51061–51074. https://doi.org/10.1007/s11356-023-25985-8

Zhu, Q., Maeno, S., Sasaki, M., Miyamoto, T., & Fukushima, M. (2015). Monopersulfate oxidation of 2,4,6-tribromophenol using an iron(III)-tetrakis(p-sulfonatephenyl)porphyrin catalyst supported on an ionic liquid functionalized Fe_3O_4 coated with silica. *Applied Catalysis B: Environmental*, *163*, 459–466. https://doi.org/10.1016/j.apcatb.2014.08.035

Zucca, P., Fernandez-Lafuente, R., & Sanjust, E. (2016). Agarose and its derivatives as supports for enzyme immobilization. In *Molecules* (Vol. 21, Issue 11). MDPI AG. https://doi.org/10.3390/molecules21111577